

# Intersubband polaritonics revisited

O. Kyriienko<sup>1</sup> and I. A. Shelykh<sup>1,2</sup>

<sup>1</sup>*Science Institute, University of Iceland, Dunhagi 3, IS-107, Reykjavik, Iceland*

<sup>2</sup>*International Institute of Physics, Av. Odilon Gomes de Lima, 1772, Capim Macio, 59078-400, Natal, Brazil*

(Dated: December 2, 2011)

We revisit the intersubband polaritonics — the branch of mesoscopic physics having a huge potential for optoelectronic applications in the infrared and terahertz domains. We show that contrary to the general opinion the Coulomb interactions play crucial role in the processes of light-matter coupling in the considered systems. We demonstrate that electron-electron and electron-hole interactions radically change the nature of the elementary excitations in these systems. We argue that intersubband polaritons represent the result of the coupling of a photonic mode with collective excitations, and not non-interacting electron-hole pairs as it was supposed in the previous works on the subject.

## I. INTRODUCTION

Intersubband optical transitions in semiconductor quantum wells (QWs) are widely used in a variety of modern optoelectronic devices operating in a broad wavelength range spanning from mid-infrared to terahertz.<sup>1–5</sup> Their practical realization needs high radiative quantum efficiency. In this context, the implementation of the concepts of strong light-matter coupling is a promising tool to improve the functionality of the devices as compare to those operating in the weak-coupling regime.<sup>6,7</sup>

The achievement of the strong coupling is possible if the absorbing media is placed inside a photonic cavity and coherent light-matter coupling overcomes the dissipative processes in the system. For intersubband transitions the experimental realization of strong coupling regime was for the first time reported in the pioneering work of D. Dini *et al.*<sup>8</sup> The elementary excitations in this case have hybrid, half-light half-matter nature and are called intersubband polaritons. They have a number of peculiarities distinguishing them from conventional cavity polaritons formed by interband excitons. First, they are formed only in TM polarization, as optical selection rules prohibit the absorption of the TE mode in intersubband transitions. Second, the strength of the coupling can be an important fraction of the photon energy, which makes possible the transition to so-called ultrastrong coupling regime<sup>2,9</sup>. The light-matter coupling constant and resulting Rabi splitting depend on the geometry of the QW and photonic cavity and the electronic density in the lowest energy subband<sup>10</sup>, which opens a possibility to tune this parameter by application of the external gate voltage.

The broad variety of the applications of intersubband polaritonics makes important the *understanding of the nature* of intersubband polaritons. The question is: what kind of the elementary excitation in a QW is coupled with a photonic mode and participate in the formation of the polariton doublet? The former can be divided into two categories: single-particle excitations (SPE) and collective excitations, appearing from electron-electron interactions and absent in the non-interacting system. The

earlier works devoted to theoretical description of the intersubband polaritons neglected Coulomb interactions completely<sup>10–13</sup> and the main qualitative conclusion was that the formation of the polaritons is a result of the coupling between non-interacting electron-hole pairs and a cavity mode. Moreover, it was claimed that bosonization approach is valid for the description of unbounded fermion pairs.<sup>13</sup>

The opinion that Coulomb effects play no substantial role in the intersubband polaritonics seems controversial, as their important role in photoabsorption of individual QWs (in the absence of a photonic cavity) is an established fact, studied extensively from both experimental and theoretical points of view.<sup>14–17</sup> Electron-electron interactions lead to the appearance of the collective excitation modes such as intersubband plasmon (ISP) which under certain conditions can give a dominant impact to the optical response.<sup>14–22</sup>

The only work considering the role of many-electron interactions for intersubband transition in the microcavity known to us is a paper by M. Pereira<sup>23</sup>. However, the influence of interactions on quasiparticle spectrum was not the main focus of the paper. The qualitative aspects of strong light-matter interaction of collective intersubband modes with microcavity photons remained uninvestigated and the role of the many-body corrections of various types thus remained unclear.

In the current paper we bridge this evident gap. We propose a semi-analytical way of the description of the coupling between intersubband excitations (single-particle or collective) to a cavity mode in terms of Feynman diagrams corresponding to the different physical processes in the system. This makes our calculations transparent and allows a simple qualitative interpretation of the role of many body interactions in the considered system. Moreover, since we sum up infinite series of the diagrams, our treatment is non-perturbative and includes all orders of the interaction. As well, it treats the resonant and anti-resonant terms in light-matter coupling Hamiltonian on equal footing and thus allows the description of the phenomenon of ultra-strong coupling as well. We show that Coulomb interactions play cru-

cial role in the intersubband polaritonics, especially for high electron concentrations necessary for the achievement of strong coupling regime. We claim that in this case the intersubband polariton is formed due to the coupling of the collective excitation known as intersubband plasmon (ISP) with the cavity mode. In the opposite case of small electron concentrations we show that excitonic corrections become crucial.

## II. THE MODEL

We consider a system with GaAs/AlGaAs quantum well (QW) embedded into microcavity in the configuration usually used for intersubband transitions with TM polarized light (Fig. 1(a,b)). As our goal here is to present qualitative results and not to perform a fit of any experimental data, we do not consider the case where the photonic cavity contains several QWs which is often used in order to obtain larger values of Rabi splitting and necessary for the achievement of the ultra-strong coupling.<sup>2,9</sup> Our method, however, can be easily generalized for this configuration as well. We choose a doping of a single QW in such a way that only the lowest subband is filled by the electrons at  $T = 0$  while upper subbands remain empty (Fig. 1(c)). Later on we concentrate on  $T = 0$  case only.

When quantum well is embedded into a microcavity, the photons interact continuously with electrons moving them from fundamental subband to the first excited subband, thus creating electrons and holes which can interact with each other. This electron-hole pairs can then again disappear, re-emitting a photon. In diagrammatic language such process can be described by a polarization bubble  $\Pi$  (Fig. 2). The photon in a cavity thus becomes "dressed" by such bubbles, and its Green function  $G$  can be described as a sum of the terms containing one, two, three *etc* bubbles as it is shown in Fig. 2(a). The summation up to the infinite order gives the Dyson equation, whose solution yields

$$G = \frac{G_0}{1 - g^2 G_0 \Pi}, \quad (1)$$

where  $\Pi$  denotes to the full polarization operator described by the intersubband bubble containing all possible Coulomb interactions. In this expression  $G_0$  is a bare photon Green function,

$$G_0(\omega, q) = \frac{2\hbar\omega_0(q)}{\hbar^2\omega^2 - \hbar^2\omega_0^2(q) + 2i\Gamma\omega_0(q)}, \quad (2)$$

where  $\omega_0(q)$  describes the cavity mode dispersion and  $\Gamma$  is the broadening of the photonic mode due to the finite lifetime (taken to be  $\approx 10ps$ ) and  $g$  is a matrix element of electron-photon interaction which reads<sup>10</sup>

$$g(q) = \sqrt{\frac{\Delta \cdot d_{10}^2}{\hbar^2\epsilon\epsilon_0 L_{cav} A \omega_0(q)} \frac{q^2}{(\pi/L_{cav})^2 + q^2}}, \quad (3)$$

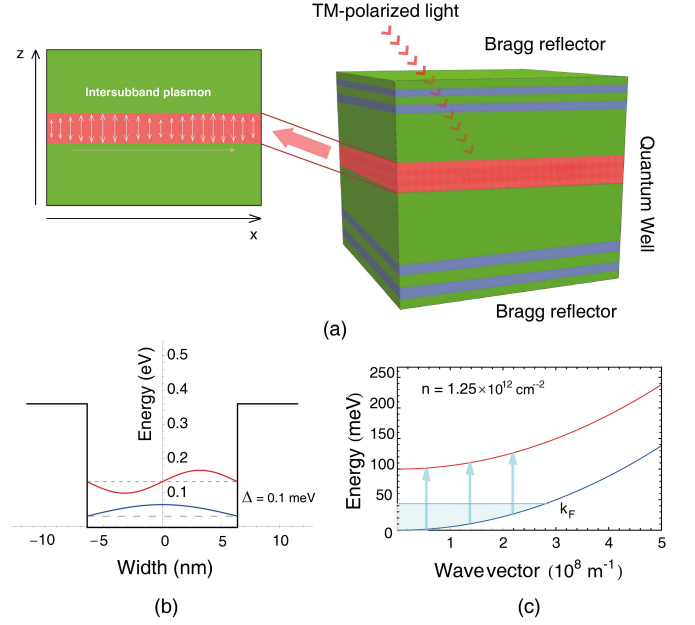


FIG. 1: (Color online) Geometry of the system. (a), GaAs quantum well (QW) placed into the microcavity created by distributed Bragg reflectors or air. Using the total internal reflection of light, TM-polarized beam travels through the structure exciting the excitations between upper and lower subbands. The current figure shows the creation of intersubband plasmon – charge-density excitation. (b), Sketch of the QW of width  $L = 12.8 \text{ nm}$  with plotted wave functions for fundamental and upper subbands. The separation energy between levels is ( $\Delta = 100 \text{ meV}$ ). (c), Dispersions of electrons for two subbands with Fermi level energy for electron concentration  $n_{el} = 1.25 \times 10^{12} \text{ cm}^{-2}$ . The single-particle excitations are schematically described as blue arrows. The  $k_F$  label denotes to the Fermi wave vector.

where  $L_{cav}$  is cavity length,  $\Delta$  is separation energy between levels,  $\epsilon_0$  and  $\epsilon$  are vacuum permittivity and relative material dielectric constant, respectively,  $d_{10}$  stands for the dipole matrix element of the transition and  $A$  is an area of the sample.

The dispersion of elementary excitation in such system is determined by the poles of  $G(\omega, q)$  and can be found by solving a transcendental equation

$$1 - g^2 G_0 \Pi = 0. \quad (4)$$

The coefficient of the photoabsorption,  $\alpha(q, \omega)$ , is proportional to the imaginary part of the full polarization operator of intersubband polariton accounting for multiple re-emissions and re-absorptions of the cavity photon  $\Pi_{pol}(q, \omega)$ :

$$\alpha(q, \omega) \sim \omega \Im \Pi_{pol}(q, \omega). \quad (5)$$

The diagrammatic representation of the equation for  $\Pi_{pol}(q, \omega)$  is shown in Fig. 2(b) and yields

$$\Pi_{pol} = \frac{\Pi}{1 - g^2 G_0 \Pi}. \quad (6)$$

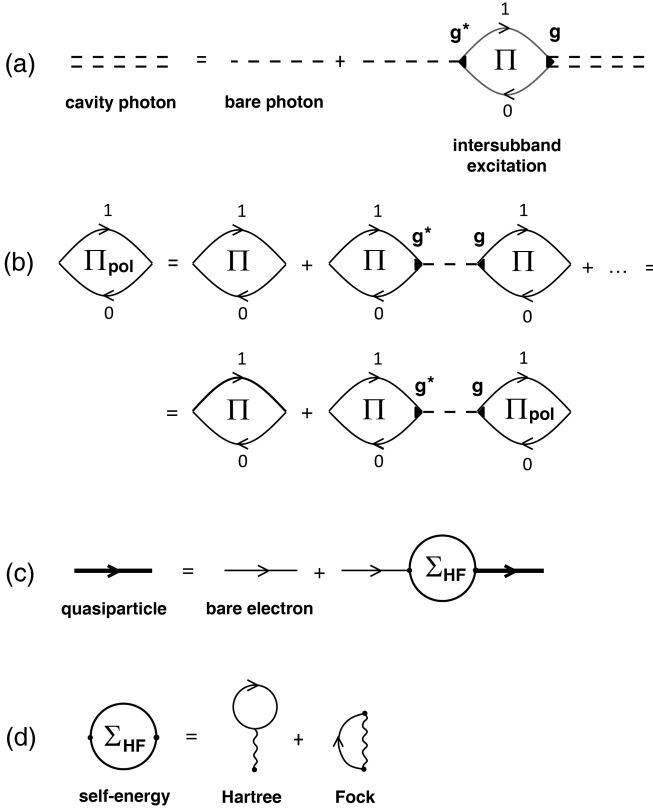


FIG. 2: Diagrammatic representation of intersubband polaritons. (a), The Dyson equation for microcavity photon interacting with intersubband quasiparticles  $\Pi$  leading to the formation of polariton. The label  $g$  corresponds to quasiparticle-photon interaction constant, indices 1 and 0 denote to excited and fundamental subband, respectively. (b), Series for absorption by intersubband quasiparticle coupled to the cavity in the general form with accounting all many-body effects. (c), The Dyson equation for self-energy corrections of the Green function of the electron. (d), The Hartree-Fock self-energy which consists of direct (Hartree) and exchange (Fock) diagrams.

As it is seen from the Eqs. (4)-(6), all properties of intersubband polaritons can be determined if the expression of the polarization operator of an individual QW  $\Pi(q, \omega)$  accounting for Coulomb interactions is known. In general, the calculation of this quantity is a tricky task which can be performed only in some particular cases, which we are now going to consider.

### III. NON-INTERACTING CASE AND HARTREE-FOCK APPROXIMATION

This case has a methodological interest and represents a test for our approach, allowing to compare the results it gives with those obtained earlier in the Refs. [10–13] by using the bosonisation scheme. For non-interacting particles the calculation of the polarization operator  $\Pi_0$  represented by a single bubble without any Coulomb in-

teractions is straightforward and gives<sup>18</sup>

$$\Pi_0(\omega, q) = 2 \int \frac{d\mathbf{k}}{(2\pi)^2} \frac{n_{0\mathbf{k}}}{\hbar\omega + E_{\mathbf{k}}^{(0)} - E_{\mathbf{k}+\mathbf{q}}^{(1)} + i\gamma}, \quad (7)$$

where  $E_{\mathbf{k}+\mathbf{q}}^{(1)} = \Delta + \hbar^2(\mathbf{k} + \mathbf{q})^2/2m$  and  $E_{\mathbf{k}}^{(0)} = \hbar^2 k^2/2m$  are dispersions of electrons in the excited and fundamental subbands, respectively, and  $n_{0\mathbf{k}}$  is the Fermi distribution in the fundamental subband which can be replaced by a step-like function at  $T = 0$ . The quantity  $\gamma$  represents a non-radiative broadening of SPE. This integral can be calculated analytically (see Appendix A). The use of Eqs. (4)-(6) allows the determination of the dispersions of the intersubband polaritons and photoabsorption of the system. It is instructive to consider the case  $\gamma \rightarrow 0$  and assume that the transferred momentum of photon  $q$  is small as compare to the Fermi momentum of the electron gas  $k_F$ . In this case, the equation for the energies of the polariton modes (4) reads

$$(\hbar\omega - \hbar\omega_0 + i\Gamma)(\hbar\omega + \hbar\omega_0 - i\Gamma)(\hbar\omega - \Delta) = 2\omega_0 n A g^2(q). \quad (8)$$

If we are outside the ultrastrong coupling regime ( $\omega_0 \gg n A g^2(q)$ ) this reduces to

$$(\hbar\omega - \hbar\omega_0 + i\Gamma)(\hbar\omega - \Delta) = n A g^2(q), \quad (9)$$

which is nothing but the equation for two coupled harmonic oscillators corresponding to a cavity mode and single-particle excitations in the QW. The dispersions of intersubband polaritons deduced from this equation coincide with those obtained in the earlier works [10–13].

One should note that in the mean field (Hartree-Fock) approximation the electron-electron corrections can be easily introduced into consideration without substantial modification of the formalism. No new collective excitations appear in this approach and the results remain qualitatively the same as for the non-interacting case. We thus consider both situations in the same section.

In diagrammatic representation the Hartree-Fock approximation results into renormalization of electron Green functions which can be described by the Dyson equation shown in Fig. 2(c). Only the first order diagrams corresponding to the direct Hartree term and exchange Fock term (Fig. 2(d)) are retained in the expression for the self-energy in this approach. The Hartree term diverges in the limit  $A \rightarrow \infty$  but is compensated by the interaction of the electrons with positive background<sup>20</sup> and the Fock exchange self-energy correction can be written in the form

$$\Sigma_{HF}^{(i)} = - \sum_{\mathbf{k}_1} V_{i00i}(|\mathbf{k} - \mathbf{k}_1|) n_{\mathbf{k}_1}, \quad (10)$$

where  $i = 0, 1$  and the index 0 corresponds to the fundamental subband and index 1 to the first excited subband,  $n_{\mathbf{k}_1}$  denotes the Fermi distribution in the fundamental band and sign “-” shows that the exchange interaction

decreases the energy.  $V_{ijkl}(q)$  denotes a matrix element of the Coulomb interaction which reads

$$V_{ijkl}(q) = \frac{e^2}{2\epsilon\epsilon_0 A q} \int dz dz' \phi_i(z) \phi_j(z') \phi_k(z') \phi_l(z) e^{-q|z-z'|} \quad (11)$$

with indices  $i, j, k$  and  $l$  corresponding to the initial and final subbands from which particles interact and  $\phi_i(z)$  being the envelope wave functions in the direction of the structure growth axis.<sup>18,24</sup>

The calculation of the polarization operator accounting for the Hartree-Fock corrections can be done by substituting the energies of bare electrons in the fundamental and first subbands by their renormalized values, calculated as

$$\tilde{E}^{(i)}(\mathbf{k}) = E^{(i)}(\mathbf{k}) + \Sigma_{HF}^{(i)}(\mathbf{k}) \quad (12)$$

This renormalization has the following consequences. First, the correction for populated fundamental subband is greater than for the empty first subband leading to the renormalization of the transition energy  $\Delta$ . Accounting for the negative sign of exchange correction, one concludes that the effective gap  $\tilde{\Delta}$  is increased. Second, in general the self-energy is a function of momentum which leads to the non-parabolicity of the renormalized dispersions and contributes to the broadening of the absorption line. For intersubband polaritons the first effect shifts the anticrossing point in the region of larger momenta (several meV in the geometry we consider) and second leads to the slight decrease of the observed Rabi splitting.

#### IV. INTERSUBBAND PLASMON-POLARITON

In general, electron-electron interactions can not be neglected and  $\Pi \neq \Pi_0$ . Their account is a complicated task. However, for high enough electron concentrations ( $n \sim 10^{12} \text{ cm}^{-2}$ ) the polarization operator can be estimated using Random Phase Approximation (RPA) whose diagrammatic representation is shown in Fig. 3(c).<sup>15,22</sup> In this regime the system demonstrates the appearance of intersubband plasmon (ISP) — charge-density collective excitation arising from intersubband transitions.

The summation of the infinite series of the diagrams represented in Fig. 3(c) allows us to obtain a compact expression for the polarization operator corresponding to ISP:

$$\Pi_{ISP} = \frac{\Pi_0}{1 - V_{1010}\Pi_0}. \quad (13)$$

The dispersion of intersubband plasmon is plotted in Fig. 3(a). The absorption by intersubband plasmon is given by imaginary part of polarization  $\Pi$  (Fig. 3(b)). One sees that the system still has an absorption peak corresponding to the single-particle excitations. However, another peak corresponding to the absorption of

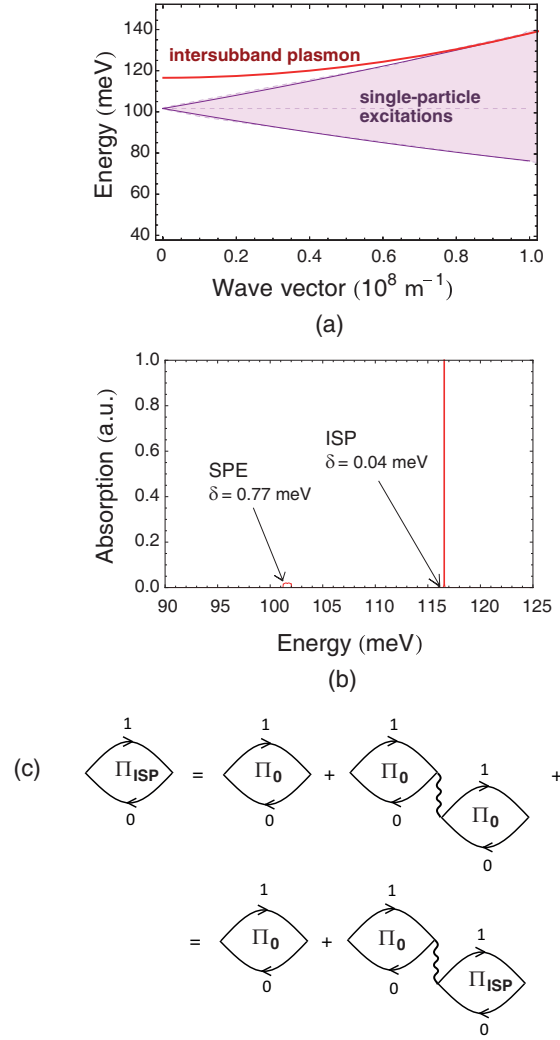


FIG. 3: (Color online) Intersubband plasmon. (a), The dispersion of intersubband plasmon (ISP, red line) and single-particle excitations spectrum (SPE, violet parabolas) plotted for the long range of momentum. For the considered concentration  $n_{el} = 1.25 \times 10^{12} \text{ cm}^{-2}$  ISP dominates over SPE in the small wave vectors range. (b), Absorption spectrum of intersubband quasiparticles plotted for momentum  $q = 10^6 \text{ m}^{-1}$ . While the intersubband plasmon peak is sharp ( $\delta = 0.05 \text{ meV}$ ) and high, the SPE continuum is much broader ( $\delta = 0.77 \text{ meV}$ ) and has smaller oscillator strength. (c), Random Phase Approximation (RPA) series for intersubband electron-hole pairs interacting by direct Coulomb matrix element  $V_{1010}$ . These diagrams correspond to the formation of intersubband plasmon.

ISP appears. This peak is blueshifted by a value of depolarization shift  $nV_{1010}(q)$ . It is much more intensive and narrow than the peak corresponding to SPE. Therefore, it is natural to suppose that after placing of the QW in a photonic cavity this peak will give main contribution to the formation of intersubband polariton.

This conclusion is supported by the results of calculations shown in Fig. 4. The dispersion of the elementary

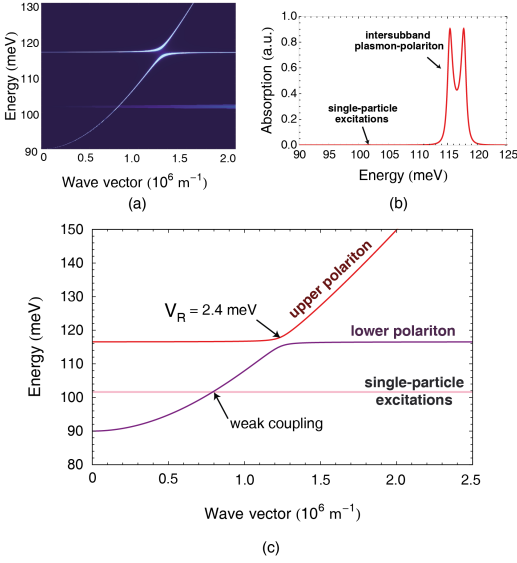


FIG. 4: (Color online) Intersubband plasmon polariton. (a), Density plot of the intersubband plasmon polariton spectrum showing the dispersion of excitations and absorption (color intensity) in the system. The detuning of cavity mode is 10 meV. (b), Absorption spectrum of the system plotted for wave vector  $q = 1.25 \times 10^6 \text{ m}^{-1}$  where the anticrossing point for ISP-photon exists. The two peaks corresponding to upper and lower plasmon polaritons are clearly observed, while single-particle excitations are suppressed. (c), Dispersions of intersubband plasmon polariton modes (red and violet lines) in strong coupling regime with corresponding anti-crossing and Rabi frequency  $V_R = 2.4 \text{ meV}$ . The SPE dispersion (pink line) is weakly coupled to the cavity mode.

excitations of the hybrid QW-cavity system was calculated using Eq. (4), where the Hartree-Fock corrections were accounted for in  $\Pi_0$ . The corresponding spectrum of intersubband excitations in the semiconductor microcavity contains three branches (Fig. 4(c)). Two of them corresponding to the cavity photons and ISP reveal anticrossing and give birth to the intersubband polariton modes, which in this case can be called more correctly intersubband plasmon-polaritons. The third mode denotes to the single-particle excitations. The corresponding dispersion line crosses the dispersion of the cavity photon, which means that for SPE the weak coupling regime is realized. In the absorption spectra shown in Fig. 4(b) three peaks appear. Two of them corresponding to intersubband plasmon-polaritons are very pronounced and the third one corresponding to coupling with single-particle excitations is very weak but still observable (Fig. 4(a)).

## V. EXCITONIC EFFECTS

In the previous section we investigated the case of high electron concentration in QW where plasmonic effects dominate and RPA can be successfully used. However, the opposite limit of low concentrations is also interest-

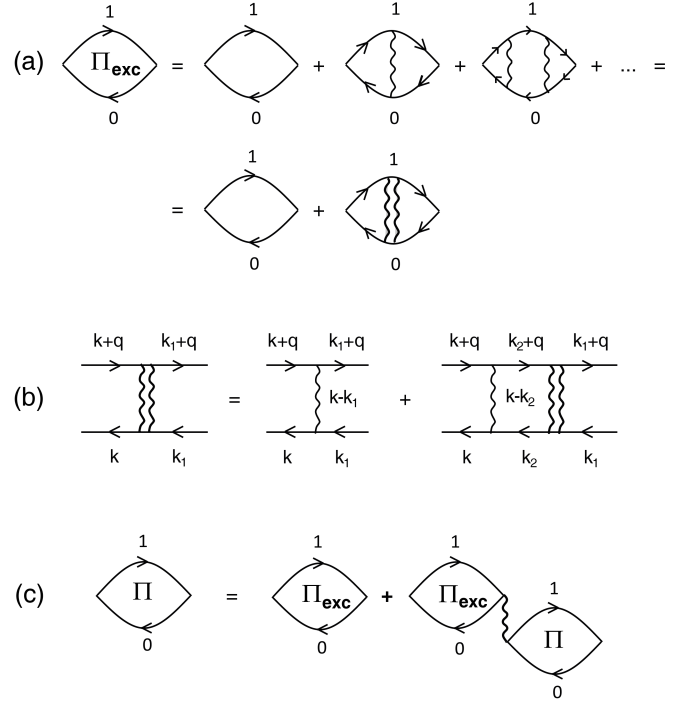


FIG. 5: Diagrammatic representation of intersubband excitation. (a), The ladder series for the intersubband excitation leading to the creation of intersubband exciton. The wavy line corresponds to  $V_{1001}$  Coulomb interaction and double wavy line denotes to effective interaction between particles. (b), Two-particle integral equation for effective interaction.  $q$  is the transferred momentum. (c), The general Dyson equation which describes the situation of mixed excitonic and plasmonic effects leading to the formation of mixed collective modes.

ing. In this case plasmonic corrections can be neglected and excitonic effects corresponding to the interaction between the photoexcited electron in the first subband with a hole in fundamental subband become dominant. In diagrammatic language they can be described by ladder diagrams shown in Fig. 5(a).<sup>25,26</sup> Summation of the ladder diagrams up to an infinite order gives birth to the formation of the attraction between the electron and hole, and can give a peak in photoabsorption lying below the continuum of SPE (contrary to the peak corresponding to ISP).

Mathematically, the dispersion of the excitonic mode can be deduced from the integral Bethe-Salpeter equation for the effective electron-hole interaction, whose diagrammatic representation is given in Fig. 5(b) and which reads<sup>25</sup>

$$W(\mathbf{k}, \mathbf{k}_1, \omega, \mathbf{q}) = -V_{1001}(\mathbf{k} - \mathbf{k}_1) - (14) \\ - \int d\mathbf{k}_2 V_{1001}(\mathbf{k} - \mathbf{k}_2) \Pi_0(\omega, \mathbf{k}_2, \mathbf{q}) W(\mathbf{k}_2, \mathbf{k}_1, \omega, \mathbf{q}).$$

The solution of the Bethe-Salpeter equation is a complicated task which goes beyond the scope of the present paper. Here we restrict ourselves by a simplified treat-

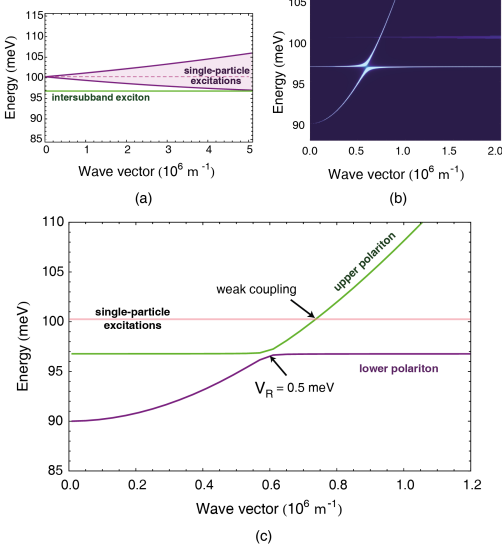


FIG. 6: (Color online) Intersubband exciton polariton. (a), The dispersion of intersubband exciton (green line) which lies below the single-particle excitations continuum (violet parabolas). The concentration of electrons in QW is  $n_{el} = 10^{11} \text{ cm}^{-2}$ . (b), Density plot of intersubband exciton coupled to the photonic mode. The intensity describes the absorption in the system. (c), Dispersions of intersubband exciton polariton modes (green and violet lines) in strong coupling regime ( $V_R = 0.5 \text{ meV}$ ). The SPE dispersion (pink line) is weakly coupled to a cavity mode.

ment of the screened 2D Coulomb potential<sup>24,27</sup>

$$V_{1001}(\mathbf{q}) \approx \frac{e^2}{2\epsilon\epsilon_0 A(|\mathbf{q}| + \kappa)}, \quad (15)$$

where  $\kappa = \frac{me^2}{2\pi\epsilon\epsilon_0\hbar^2}$  is the screening wave vector. In 2D systems it does not depend on electron density and for the structure we consider is equal to  $\kappa = 2.4 \times 10^8 \text{ m}^{-1}$ . Then, since we are working with zero temperatures and small concentrations ( $k_F < \kappa$ ), the interaction between particles is slowly varying function of  $q$  and can be approximated by a constant value  $V_0 \approx e^2/2\epsilon\epsilon_0 A\kappa$ . In this limit the equation for the polarization operator corresponding to the intersubband exciton can be found analytically as<sup>15</sup>

$$\Pi_{exc} = \frac{\Pi_0}{1 + V_0\Pi_0}, \quad (16)$$

where the negative sign of Coulomb interaction corresponding to the electron-hole attraction is accounted for in the denominator. The calculated dispersion of intersubband exciton is shown in Fig. 6(a) for the QW with doping  $n_{el} = 10^{11} \text{ cm}^{-2}$ , where assumption  $k_F < \kappa$  is appropriate.

The dispersion of the elementary excitations of the QW coupled to a cavity mode accounting for the excitonic effects are shown in Fig. 6(c). Similarly to the case of the

high concentrations with the strong ISP-photon coupling, one sees three dispersion branches. Two of them corresponding to the excitonic and photonic modes reveal anticrossing and form the intersubband exciton polaritons. The third one corresponding to single-particle excitations remains in a weak coupling regime. In the photoabsorption spectrum shown in Fig. 6(b) three peaks of different intensities are observed. The excitonic effects lead to the redistribution of the oscillator strength, which becomes small for SPE transitions and corresponding peak is consequently very weak. In this case the Rabi splitting is reduced due to the concentration dependence of interaction constant and is about 0.5 meV.

One should also comment on the case of the intermediate densities, where strictly speaking neither RPA nor ladder approximation can be applied. In some works<sup>20</sup> RPA and ladder corrections were accounted simultaneously to describe the Coulomb correlations in this regime. In the diagrammatic representation this results into the equation for the polarization operator shown in Fig. 5(c) which leads to the appearance in the system of some mixed collective exciton-plasmon modes. As depolarization and excitonic shifts have opposite signs, it may be possible that there exists a regime when they almost compensate each other and the energy of the collective mode is close to the energy of the single-particle transition. The consideration of this case, however, goes beyond the scope of the present paper.

## VI. CONCLUSIONS

In conclusion, we analyzed the elementary excitations arising from the strong coupling of a photonic cavity mode with an intersubband transition of a single QW. We have shown that contrary to the current opinion Coulomb interactions can play crucial role in the system and lead to the qualitative changes of the nature of intersubband polaritons. We predict theoretically that strong coupling of the cavity mode occurs with collective excitations, while single-particle excitations remain in the weak coupling regime.

This work was supported by Rannis "Center of Excellence in Polaritonics" and FP7 IRSES project "POLAPHEN". I.A.S. acknowledges the support from COST POLATOM program. O.K. acknowledges the help of Eimskip Foundation.

### Appendix A: Calculation of a polarization operator for non-interacting particles

The generic form of the electron-hole polarization operator for non-interacting particles can be written as

$$i\Pi_0(\omega, \mathbf{q}) = 2 \int \frac{d\mathbf{k}d\nu}{(2\pi)^4} G(\mathbf{k} + \mathbf{q}, \nu + \omega) G(\mathbf{k}, \nu), \quad (A1)$$

where  $G(\mathbf{k}, \nu)$  denotes the Green function of particle with momentum  $\mathbf{k}$  and energy  $\nu$ .  $\mathbf{q}$  and  $\omega$  correspond to the transferred momentum and energy, respectively. For the intersubband transition case the polarization bubble describes the excitation process where electron is transferred to the upper subband while the hole is created in the lower subband. Thus, the Eq. (A1) can be represented as

$$\Pi_0(\omega, q) = 2 \int \frac{d\mathbf{k}}{(2\pi)^2} \frac{n_{0\mathbf{k}}}{\hbar\omega + E_{\mathbf{k}}^{(0)} - E_{\mathbf{k}+\mathbf{q}}^{(1)} + i\gamma}, \quad (\text{A2})$$

where  $E_{\mathbf{k}+\mathbf{q}}^{(1)} = \Delta + \hbar^2(\mathbf{k} + \mathbf{q})^2/2m$  and  $E_{\mathbf{k}}^{(0)} = \hbar^2 k^2/2m$  are dispersions of electrons in the excited and fundamental subbands, respectively,  $\Delta$  is an energy distance between subbands and  $n_{0\mathbf{k}}$  is the Fermi distribution in the fundamental subband which can be replaced by a step-like function at  $T = 0$ . Parameter  $\gamma$  describes the lifetime of the excitation.

First, let us rewrite Eq. (A2) in the following form

$$\Pi_0(\omega, q) = 2 \int_0^{k_F} \frac{k dk}{(2\pi)^2} \int_0^{2\pi} \frac{d\phi}{\hbar\omega - \Delta - \hbar^2 q^2/2m - \hbar^2 k q \cos \phi/m + i\gamma}, \quad (\text{A3})$$

where  $\phi$  is an angle between two vectors  $\mathbf{k}$  and  $\mathbf{q}$ . The assumption that transferred momentum of photon  $q$  is small yields simple integration on  $\phi$  and  $k$ , and the real part of polarization operator is

$$\Re \Pi_0(\omega)_{q \rightarrow 0} = \frac{nA}{\hbar\omega - \Delta}, \quad (\text{A4})$$

where  $n = \frac{k_F^2}{2\pi}$  is 2D density of electron gas,  $A$  is QW area and we assumed  $\gamma \rightarrow 0$ .

Now we return to the case of non-negligible photon momentum and calculate the imaginary part of polarization operator (A3). The analysis of the denominator shows that integral on  $k$  in Eq. (A3) has poles only in certain angular range  $[\phi_{min}, \phi_{max}]$ :

$$\arccos \left[ \frac{(\hbar\omega - \Delta - E_q)}{\hbar^2 k_F q/m} \right] < \phi < \arccos \left[ \frac{-(\hbar\omega - \Delta - E_q)}{\hbar^2 k_F q/m} \right]. \quad (\text{A5})$$

Thereby, in this region one can find the imaginary part of polarization operator using residue theorem in the limit  $\gamma \rightarrow 0$ :

$$\Im \Pi_0(\omega, q)_{\gamma \rightarrow 0} = \frac{Am}{4\hbar^2} \frac{1}{E_q} (\hbar\omega - \Delta - E_q) \tan \phi|_{\phi_{min}}^{\phi_{max}} \equiv I_\delta(\omega, q), \quad (\text{A6})$$

which describes a peak in the region where single-particle excitations exist, bounded by parabolas  $\Delta + \hbar^2 q^2/2m - \hbar^2 k_F q/m$  and  $\Delta + \hbar^2 q^2/2m + \hbar^2 k_F q/m$ .

However, to describe the realistic absorption spectral function one needs to account for the finite non-radiative lifetime of intersubband excitations. It can be done using the Sokhatsky-Weierstrass theorem with non-zero  $\gamma$

$$\int \frac{f(x)}{x + i\gamma} dx = -i\pi \int \frac{\gamma f(x)}{\pi(x^2 + \gamma^2)} dx + \int \frac{x f(x)}{(x^2 + \gamma^2)} dx. \quad (\text{A7})$$

The integral (A3) can be rewritten in the similar form

$$\begin{aligned} \Pi_0(\omega, q) &= -2 \int_0^{2\pi} \frac{d\phi}{(2\pi)^2} \int_0^{k_F} \frac{k}{Bk + C + i\gamma} dk = (\text{A8}) \\ &= -\frac{1}{2\pi^2} \int_0^{2\pi} \frac{d\phi}{B} \int_0^{k_F} \frac{k}{k - k_0 + i\gamma} dk = \\ &= -\frac{1}{2\pi^2} \int_0^{2\pi} \frac{d\phi}{B} \int_{-k_0}^{k_F - k_0} \frac{\tilde{k} + k_0}{\tilde{k} + i\gamma} d\tilde{k}, \end{aligned}$$

where  $B = \hbar^2 q \cos \phi/m$ ,  $C = \hbar\omega - \Delta - \hbar^2 q^2/2m$ ,  $k_0 = C/B$  and the  $\phi$ -dependence of  $B$  and  $k_0$  should be taken into consideration. In the latest expression the new integration variable  $\tilde{k} = k - k_0$  was used. Thus, comparing the Eqs. (A8) and (A7), one can calculate numerically the imaginary part of polarization operator (A3) with finite lifetime of excitations. One sees that integral (A8) can be separated into two parts. Detailed analysis shows that the first integral gives obtained previously delta-function like absorption which does not depend on  $\gamma$ , while the second integral  $I_{Lor}$  is proportional to  $\gamma$  and has Lorentzian form. Therefore, for the sake of simplicity, in the purely analytical calculations it is possible to use absorption spectrum as the sum of equation (A6) and phenomenological Lorentzian broadening due to finite lifetime of excitation ( $\tau \approx \mu s$ ) written in the form<sup>24</sup>

$$I_{Lor}(\omega) = \Im \left[ \frac{nA}{\hbar\omega - \Delta + i\gamma} \right] = \frac{-\gamma nA}{(\hbar\omega - \Delta)^2 + \gamma^2}. \quad (\text{A9})$$

Finally, the imaginary part of polarization operator which describes optical absorption by intersubband transition yields

$$\Im \Pi_0(\omega, q) = I_\delta(\omega, q) + I_{Lor}(\omega) \quad (\text{A10})$$

The real part of polarization operator can be found by direct integration in Eq. (A3)<sup>18,24</sup>

$$\begin{aligned} \Re \Pi_0(\omega, q) &= \frac{Am}{\pi \hbar^2} \frac{1}{2E_q} ((\hbar\omega - \Delta - E_q) \mp \\ &\mp \sqrt{(\hbar\omega - \Delta - E_q)^2 - 4E_F E_q}), \end{aligned} \quad (\text{A11})$$

where " - " sign corresponds to the case  $\hbar\omega > \Delta$  and " + " for  $\hbar\omega < \Delta$ .

Consequently, the polarization operator  $\Pi_0$  which stands for the simple intersubband bubble is described by the sum of real (Eq. (A11)) and imaginary (Eq. (A10)) parts. Finally, using it in the Dyson equations, the optical response and elementary excitation spectrum can be found.

- 
- <sup>1</sup> E. Dupont, H. C. Liu, A. J. SpringThorpe, W. Lai, and M. Extavour, Phys. Rev. B **68**, 245320 (2003).
  - <sup>2</sup> G. Gunter, A. A. Anappara, J. Hees, A. Sell, G. Biasiol, L. Sorba, S. De Liberato, C. Ciuti, A. Tredicucci, A. Leitenstorfer, R. Huber, Nature Lett. **458**, 07838 (2009).
  - <sup>3</sup> C. Walther, M. Fischer, G. Scalari, R. Terazzi, N. Hoyler, and J. Faist, Appl. Phys. Lett. **91**, 131122 (2007).
  - <sup>4</sup> O. Cathabard, R. Teissier, J. Devenson, J. C. Moreno, and A. N. Baranov, Appl. Phys. Lett. **96**, 141110 (2010).
  - <sup>5</sup> D. Oustinov, N. Jukam, R. Rungsawang, J. Madeo, S. Barbieri, P. Filloux, C. Sirtori, X. Marcadet, J. Tignon, and S. Dhillon, Nat. Commun. 1:69 doi: 10.1038/ncomms1068 (2010).
  - <sup>6</sup> R. Colombelli, C. Ciuti, Y. Chassagneux, C. Sirtori, Semicond. Sci. Technol. **20**, 985 (2005).
  - <sup>7</sup> P. Jouy, A. Vasanelli, Y. Todorov, L. Sapienza, R. Colombelli, U. Gennser, and C. Sirtori, Phys. Rev. B **82**, 045322 (2010).
  - <sup>8</sup> D. Dini, R. Kohler, A. Tredicucci, G. Biasiol, and L. Sorba, Phys. Rev. Lett. **90**, 116401 (2003).
  - <sup>9</sup> Y. Todorov, A. M. Andrews, R. Colombelli, S. De Liberato, C. Ciuti, P. Klang, G. Strasser, and C. Sirtori, Phys. Rev. Lett. **105**, 196402 (2009).
  - <sup>10</sup> S. De Liberato and C. Ciuti, Phys. Rev. B **77**, 155321 (2008).
  - <sup>11</sup> C. Ciuti, G. Bastard, I. Carusotto, Phys. Rev. B **72**, 115303 (2005).
  - <sup>12</sup> C. Ciuti and I. Carusotto, Phys. Rev. A **74**, 033811 (2006).
  - <sup>13</sup> S. De Liberato and C. Ciuti, Phys. Rev. Lett. **102**, 136403 (2009).
  - <sup>14</sup> A. Pinczuk, S. Schmitt-Rink, G. Danan, J. P. Valladares, L. N. Pfeiffer, and K. W. West, Phys. Rev. Lett. **63**, 1633 (1989).
  - <sup>15</sup> I. K. Marmorkos and S. Das Sarma, Phys. Rev. B **48**, 1544 (1993).
  - <sup>16</sup> O. E. Raichev and F. T. Vasko, Phys. Rev. B **60**, 777 (1999).
  - <sup>17</sup> M. F. Pereira and H. Wenzel, Phys. Rev. B **70**, 205331 (2004).
  - <sup>18</sup> J. Dai, M. E. Raikh, and T. V. Shahbazyan, Phys. Rev. Lett. **96**, 066803 (2006).
  - <sup>19</sup> S. Das Sarma and I. K. Marmorkos, Phys. Rev. B **47**, 16343 (1993).
  - <sup>20</sup> D. E. Nikonov, A. Imamoglu, L. V. Butov, and H. Schmidt, Phys. Rev. Lett. **79**, 4633 (1997).
  - <sup>21</sup> J. Li and C. Z. Ning, Phys. Rev. Lett. **91**, 097401 (2003).
  - <sup>22</sup> J. C. Ryan, Phys. Rev. B **43**, 12406 (1991).
  - <sup>23</sup> M. F. Pereira, Phys. Rev. B **75**, 195301 (2007).
  - <sup>24</sup> H. Haug and S. W. Koch, *Quantum Theory of the Optical and Electronic Properties of Semiconductors* (World Scientific, Singapore, 1990).
  - <sup>25</sup> O. Betbeder-Matibier and M. Combescot, Eur. Phys. J. B **22**, 17-29 (2001).
  - <sup>26</sup> G. D. Mahan, *Many Particles Physics* (Plenum Press, New York, 1993).
  - <sup>27</sup> M. E. Portnoi and I. Galbraith, Solid State Commun. **103**, 325-329 (1997).